2

Embryology, Anatomy, and Pathology of Ventricular Outflow Tracts Related to Cardiac Mapping and Arrhythmias

Bastiaan J.D. Boukens[1], Cristina Basso[2], Federico Migliore[2], Stefania Rizzo[2], and Gaetano Thiene[2]

[1] *Department of Medical Biology, Academic Medical Center, Amsterdam UMC, Amsterdam, The Netherlands*
[2] *Department of Cardiac, Thoracic, and Vascular Sciences, University of Padua Medical School, Padova, Italy*

Summary

Ventricular arrhythmias, especially those of non-ischemic heart diseases, arise mostly from the outflows. Differences in embryonic origin and phenotype may account for arrhythmogenic propensity of right ventricular outflow tract (RVOT). The anatomy of the ventricles may be divided into inflow, apex, and outflow. As far as RVOT (pulmonary infundibulum) is concerned, it goes from the moderation band to the semilunar pulmonary valves. Since some myocardium extends distally from the "nadir" of the valve ring, arrhythmias may originate from the "pulmonary artery." This is true also on the aortic side, where the myocardium located within the coronary Valsalva sinuses may be the source of "aortic" arrhythmias. Arrhythmias with substrate from the RVOT may be genetically determined (arrhythmogenic cardiomyopathy), immune mediated (sarcoidosis) or infective (viral myocarditis), or form without substrate (idiopathic RVOT tachycardia). It is still controversial whether Brugada syndrome occurs in normal hearts or presents a substrate at the infundibular level.

Electroanatomical mapping plays a crucial role in establishing the existence of lacking electrical activity ("electric scars"), but it is unable to establish the precise nature of the underlying disease. Endomyocardial biopsy in this setting is the gold standard for diagnosis.

Introduction

Sudden cardiac death accounts for 300 000 deaths per year in the USA [1] and up to 5% are due to arrhythmias related to genetic abnormalities [2]. Many of these arrhythmias originate in the right ventricle (RV) and, in particular, the right ventricular outflow tract (RVOT) [3,4]. Although the mechanisms underlying these arrhythmias have been thoroughly investigated over the last 15 years, several aspects remain insufficiently understood. In particular, it is still unclear why the RVOT is the preferential site of origin of these arrhythmias. Animal studies show that during embryonic heart development, the RVOT forms from the embryonic outflow tract (OFT) [5] which, in contrast to the developing ventricles, has slow-conducting properties [6]. The OFT is in turn derived from a pool of cardiac precursor cells that differs from those of the left ventricle (LV) [7]. The differences in embryonic origin and phenotype between the LV and RV may provide insight into the arrhythmogenic nature of the RVOT [8].

Development of the outflow tract

Early development of the embryonic outflow tract

Studies in mice and chickens have shown that the heart forms from a pool of cardiac precursor cells located in a crescent-shaped field. The heart field can be divided into progenitor cells, that are located laterally in the embryo and differentiate early into myocardium (referred to as the first heart field) [7], and cells that are located medially and caudally and differentiate later during cardiac development (referred to as the second heart field).

The cells from the first heart field fuse at the midline and form a tube. This early heart tube is composed of primary (embryonic) myocardium and has an inflow tract and an OFT interconnected at the dorsal side by the fusing mesocardium. The early heart tube grows by recruitment of progenitor cells of the second heart field, which are added at the inflow tract, OFT, and dorsal mesocardium. During this elongation phase, the heart tube loops and ventricular working myocardium differentiates at the ventral side and atrial working myocardium at the dorsal side of the tube [9]. The chambers expand by rapid proliferation of the differentiating myocytes, whereas the parts flanking the chambers, the atrioventricular (AV) canal, the OFT, and the inner curvature, neither proliferate nor expand, and do not differentiate into working myocardium [9].

The LV starts to differentiate first, followed by the RV, which differentiates and expands cranially of the LV.

Cardiac Mapping, Fifth Edition. Edited by Mohammad Shenasa, Gerhard Hindricks, David J. Callans, John M. Miller, and Mark E. Josephson.

Companion website: www.wiley.com/go/cardiacmapping5e

Because these structures are formed subsequently, the progenitor cells of these three compartments have a different developmental history and have been exposed to different signals and gene programs prior to their differentiation [10]. In the embryonic heart, the OFT extends at the outer curvature from the RV to the pericardial cavity and at the inner curvature from the LV (here connected to the AV canal) to the pericardial cavity. At this stage, the OFT myocardium still retains its primary myocardial phenotype – slow conduction and low contractility – while the LV and RV acquire the working myocardial phenotype – fast conduction and high contractility (Figure 2.1).

Transition from embryonic outflow tract to left and right ventricular outflow tracts

Since the embryonic OFT is commonly defined as the tubular structure connecting the embryonic RV with the pericardial deflection, its cell composition changes immensely over time. This is because during development, cells from the pharyngeal mesoderm pass through the embryonic OFT towards the RV, enabling ventricular growth [11]. At 28–32 days of human development (embryonic), the OFT fully consists of myocardial cells. Further in development, the distal part will become composed of non-myocardial

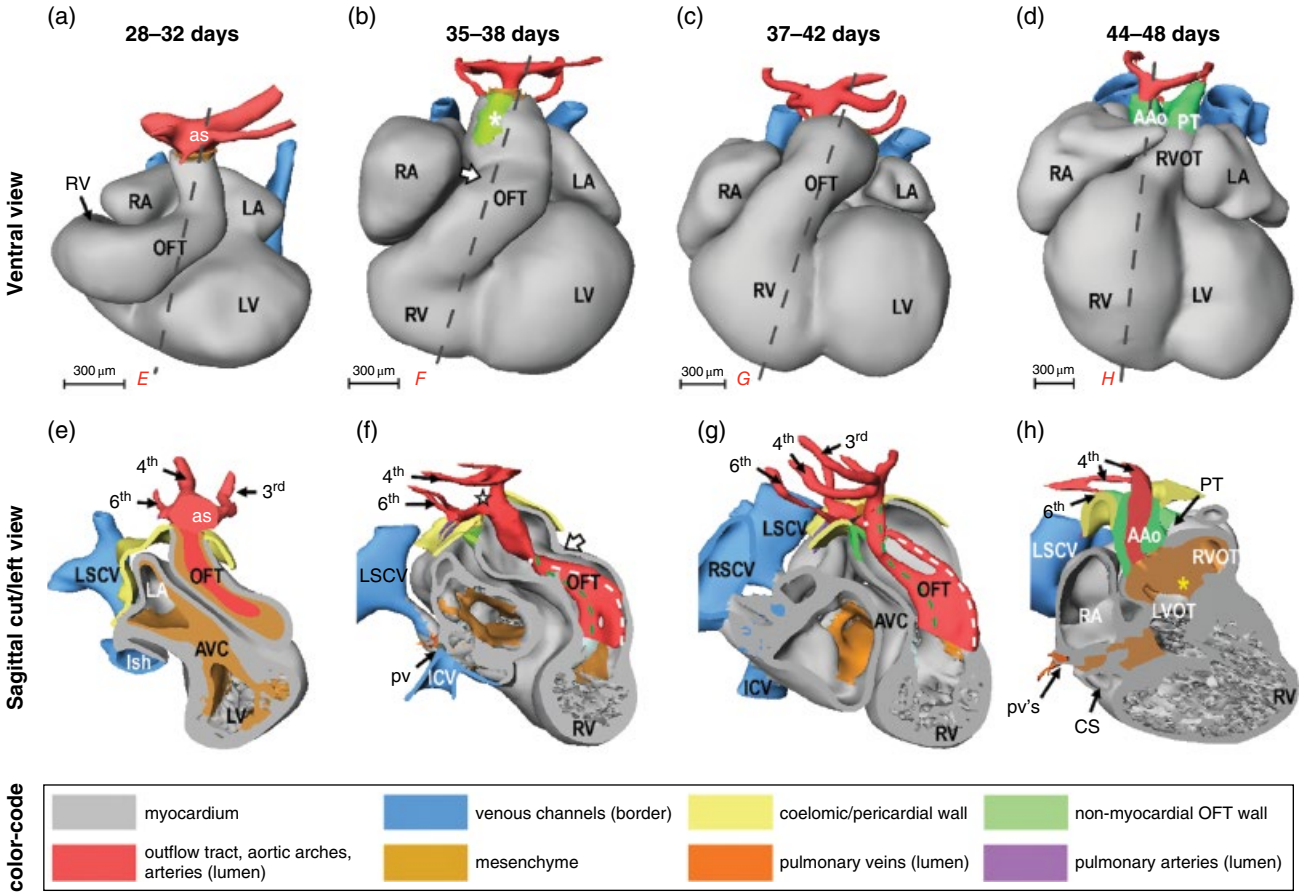

Figure 2.1 The developing outflow tract of the human heart. (a) At this stage the myocardial outflow tract (OFT), connecting the right ventricle with the aortic sac (as), is tubular. The 3rd, 4th, and 6th aortic arches originate directly from the aortic sac. (b) The intrapericardial mesenchymal tissue forming the column-like structures at the ventral and dorsal aspects of the distal outflow tract (asterisks in (a)). (c) The muscular outflow tract has further shortened, and the mass of the right ventricle is ventrally recognizable. The extrapericardial portions of the perpendicularly oriented ascending aorta and pulmonary trunk are separated from each other by mesenchymal tissue. (d) The myocardial outflow tract has further shortened, along with formation of the right ventricular infundibulum (RVOT). The intrapericardial ascending aorta and pulmonary trunk now possess their own discrete non-myocardial walls. The arrows in (b) and (f) point to the characteristic bend of the myocardial outflow tract, dividing it into proximal and distal parts. Dotted lines in (f) refer to the spirally oriented channels in the proximal outflow tract connecting the unseptated distal outflow tract with the right ventricle (*white line*) and the primary interventricular foramen (*green line*). (g) The relations between the developing ascending aorta and pulmonary trunk (*white and green dotted lines, respectively*) now resemble the situation seen in the formed heart. The asterisk in (h) refers to the myocardializing mesenchyme between the ventricular outflow tracts. *Source:* Modified from Sizarov et al. [12] with permission of John Wiley & Sons. AVC, atrioventricular canal; e/tr, (undivided) developing esophagus and trachea; LA/RA, left/right atrium; LSCV, left superior cardinal vein; lsh, left sinus horn; LV/RV, left/right ventricle; SV, sinus venosus; pv, pulmonary vein; tr, trachea; cs, coronary sinus.

cells, which will later, after septation, give rise to the intrapericardial aortic and pulmonary components [12,13]. The proximal part of the embryonic OFT will ventricularize and be incorporated into the ventricular free wall and form the left ventricular outflow tract (LVOT) and RVOT, respectively.

Thus, the RVOT and LVOT have a common origin, which may point to a common mechanism underlying outflow tract arrhythmias. Interestingly, however, the inferior part of the embryonic OFT gives rise to the subpulmonary myocardium (corresponding to the RVOT), and the superior part to the subaortic myocardium (corresponding to the LVOT). These two parts show differential gene expression (e.g. inferior part expresses *Sema3C*) and the subpulmonary myocardium is specifically affected and possibly largely absent in Tbx1 mutant mice [14]. Therefore, the RVOT and LVOT are not molecularly identical, but both are different from the LV and RV. The RVOT and LVOT acquire the working myocardial phenotype just before birth [15].

Developmental basis for RVOT arrhythmias

Electrophysiological characteristics of the RVOT

Conduction in the myocardium depends on the availability of sodium (Na^+) channels (encoded by *SCN5A*) and intercellular electrical coupling by gap junctions, which are formed by connexin (Cx) subunits. In the developing human working myocardium, the expression of *SCN5A*, *CX40*, and *CX43* is high [16], which results in relatively fast conduction (±20 cm/s) [6]. In the embryonic OFT, however, the expression of *SCN5A* is low and the expression of *Cx40* and *Cx43* is absent, resulting in slow conduction (±1–5 cm/s) [6]. Accordingly, myocytes isolated from the embryonic OFT have a slower upstroke velocity and a less depolarized resting membrane potential than myocytes from the RV or LV [17,18].

During the fetal stage of development, the embryonic OFT is fully incorporated into the RV myocardium and forms the RVOT and LVOT. In the fetal RVOT, conduction is faster (±5–10 cm/s) than in the embryonic OFT (±1–5 cm/s). However, it still remains slower than in the working myocardium (±40 cm/s) [15]. The expression of *Cx43* is maintained in the ventricles, but remains absent from the RVOT. In the adult heart, the *Cx43*-negative myocardium only remains present just below the pulmonary valves, thereby resembling the ring of primary myocardium that is present at the entrance of the RV and LV [19,20]. Primary myocardium is spontaneously active and is often, although incorrectly, referred to as nodal myocardium. These primary myocardial cells could give rise to spontaneous activity.

In the adult heart, the expression of Cx43 is lower in the RVOT than in the remainder of the heart. Despite this, the conduction velocity in the adult RVOT is not slower than in the remaining RV (±40 cm/s in both). The low expression of *Cx43* and *SCN5A* in the RVOT, however, indicates a lower safety factor [21] for conduction than in the RV. Indeed, when the safety factor of cardiac conduction is decreased pharmacologically (sodium channel blockade) or genetically (heterozygous mutation in *SCN5A*), conduction becomes slower in the RVOT than in the RV or LV [15]. This suggests that, at least in mice, this aspect of the slowly conducting embryonic OFT is retained in the free wall of the adult RVOT (Figure 2.2).

Predisposition of the RVOT to arrhythmias

Arrhythmias originating predominantly in the RVOT include idiopathic outflow tract tachycardia, Brugada syndrome, and, to a lesser extent, arrhythmogenic cardiomyopathy. Arrhythmias in these cardiac pathologies usually do not occur at a pediatric age but rather in young adulthood, indicating that postnatal development and maturation play an important role in disease development. The electrophysiological characteristics of the RVOT, however, develop prenatally and are different from those of the LV and RV [15]. The developmental history and phenotype of the RVOT are not intrinsically arrhythmogenic, but may predispose to arrhythmias in the setting of an active pathological mechanism that progresses during life.

Brugada syndrome

The Brugada syndrome is characterized by ST segment elevation in the right precordial leads and highly fractionated local electrograms in the RVOT and ventricular arrhythmias [22–26]. The mechanism underlying these characteristics is debated, but evidence supporting conduction delay or block as a potential mechanism is accumulating. In 20–30% of Brugada syndrome patients, a loss of function mutation in *SCN5A* has been found [24]. A reduction in the Na + current itself, however, does not lead to Brugada characteristics [26a]. In contrast, reducing the Na + current is used to discriminate between patients who have Brugada syndrome and those who do not [24]. In patients with Brugada syndrome, subtle, small structural discontinuities have been demonstrated in the RV free wall and RVOT [23,27,28]. Experimental and clinical studies have shown that conduction can be delayed in the myocardium with small structural discontinuities or even be blocked by a mechanism called current-to-load mismatch [29,30]. Conduction block is a prerequisite for reentry and may generate a substrate for reentrant-based arrhythmias as seen in Brugada syndrome patients [27].

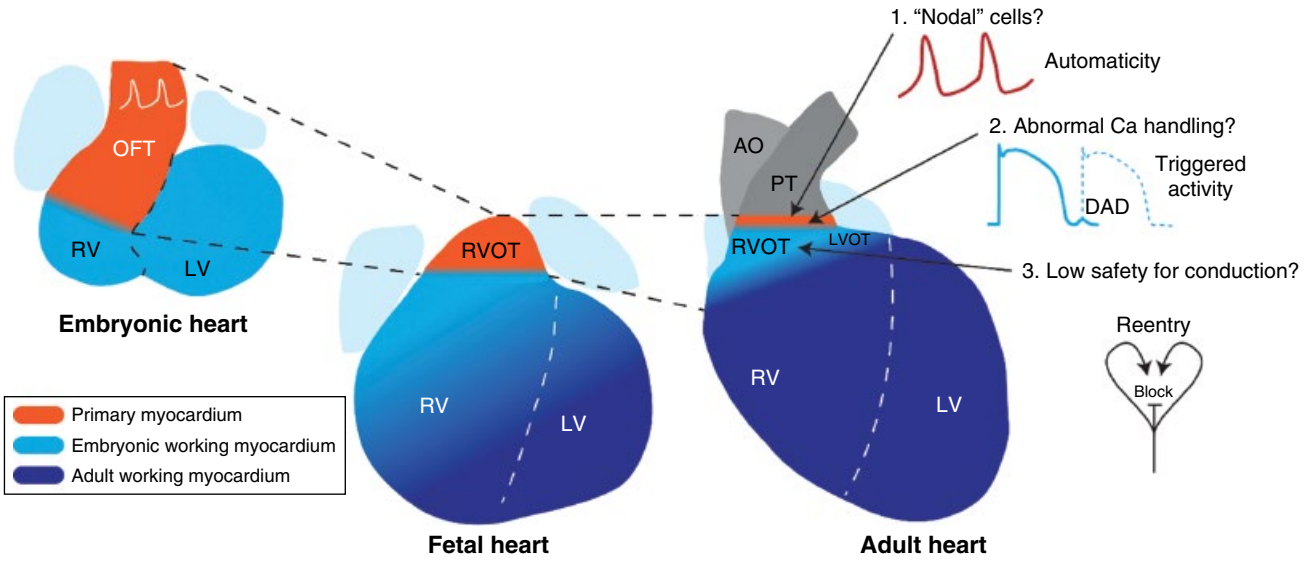

Figure 2.2 Developmental basis for RVOT arrhythmias. The adult RVOT has formed from the embryonic outflow tract (*left*), which is composed primarily of the myocardium exhibiting slow conduction and spontaneous activity. During development, the embryonic outflow tract acquires a working myocardial phenotype, e.g. fast conduction, and transforms into the RVOT. A small ring of primary myocardium, however, still remains just below the pulmonary valve which may give rise to automaticity as seen in patients with idiopathic RVOT tachycardia. The myocardium of the free wall and septum of the adult RVOT has a working myocardial phenotype, although expression of *Cx43* and *SCN5A* is lower than in the right ventricle. This may set the stage for reentrant-based arrhythmias as seen in patients with the Brugada syndrome. LV, left ventricle; OFT, outflow tract; RV, right ventricle; RVOT, right ventricular outflow tract.

In addition, conduction delay or block can cause ST segment elevation on the body surface electrocardiogram (ECG), which is a hallmark of Brugada syndrome [31,32].

Although a unifying mechanism explaining arrhythmias in Brugada syndrome patients has been proposed [32], it does not offer an explanation for the preferential location of these arrhythmias in the RVOT. We thus surmise that genes of the ventricular working myocardial genetic program are less active in the RVOT, resulting in a reduced safety of conduction, thereby facilitating current-to-load mismatch and subsequently arrhythmias. Indeed, lower expression of Cx43 protein has been found in the epicardial region of the RVOT when compared to the RV in patients with Brugada syndrome [33].

Idiopathic outflow tract tachycardias

The mechanism underlying idiopathic RVOT tachycardias is, by definition, unknown. However, these arrhythmias are catecholamine sensitive, suggesting automaticity or triggered activity as an underlying mechanism. Indeed, idiopathic arrhythmias can be treated with adenosine or beta-blockers [4]. A subset of myocytes in the RVOT have long action potentials, do not depolarize fully to the resting membrane potential, and easily develop early afterdepolarizations [34]. This electrophysiological phenotype is expected from the primary ring myocardium that is present just below, and above, the valves of the pulmonary artery. These primary myocytes may, in the presence of structural changes or uncoupling, give rise to spontaneous activity [19,35]. Consistently, ectopic beats in the RVOT are reported to originate from the myocardium just below the pulmonary valve and even from myocardial sleeves in the pulmonary artery [36,37]. For the moment, however, the direct relation between these primary cells and idiopathic RVOT tachycardia remains elusive and further research is required to determine a causal relation.

Anatomy of the right ventricle

The RV is the chamber between the tricuspid AV valve and pulmonary semilunar cusps, located anteriorly and right sided, just underneath the sternum. When seen from outside, it is easily identifiable, being located on the right between the anterior and posterior interventricular grooves, where the anterior and posterior descending coronary arteries and great cardiac vein and middle cardiac vein run, respectively. The shape is triangular, with the base corresponding to the AV sulcus and the pulmonary valve orifice, and the apex distally.

The RV is a coarse trabeculated chamber, which may be divided in three parts: inflow, apex, and outlet (Figure 2.3). The inflow corresponds to the part which hosts the tricuspid valve apparatus, from the AV ring to the base of papillary muscles. The outlet, known also as the pulmonary infundibulum, is the part of the RV which goes from the moderator band and the sigmoid pulmonary valves. The apical segment is what remains distally up to the apex.

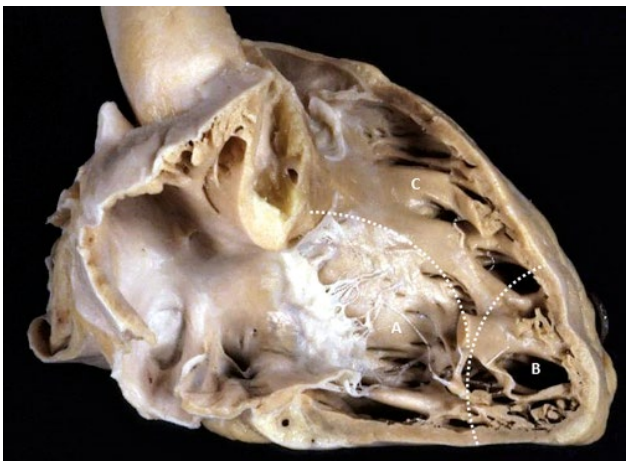

Figure 2.3 The tripartite, coarsely trabeculated right ventricle. A, Inflow, hosting the tricuspid valve. B, Apex. C, Outflow from the moderator band to the pulmonary valve.

Tricuspid valve

The tricuspid valve is a complex valvular structure which, despite being called AV because it is interposed between the atrium and ventricle, is a ventricular structure like the mitral valve, both anatomically and embryologically. It consists of three leaflets (tri-cuspid). The base of the septal leaflet is attached to the septal AV junction and goes from the anteroseptal to the posteroseptal commissures. The anteroseptal commissure corresponds to the area of the membranous septum and is indicated by fan-like chordae tendinae originating from the so-called Lancisi (conal) papillary muscle attached to the ventricular septum. The posteroseptal commissure is indicated by fan-like chordae arising from the group of posterior papillary muscles. A peculiar feature of the tricuspid valve consists in the attachment of the septal leaflet to the ventricular septum by chordae tendinae, directly or mediated by tiny papillary muscles.

The anterior leaflet is a large curtain in between the anteroseptal and anteroposterior commissures. The latter is indicated by the anterior papillary muscle, a long pillar from the tip of which chordae tendinae arise to join both the anterior and posterior leaflets, including the fan-like chordae for the anteroposterior commissure. The base of the anterior leaflet is attached to the AV ring of the anterior free wall. The difference between the anterior mitral valve leaflet and the anterior leaflet of the tricuspid valve is that the latter is not in fibrous continuity with the pulmonary semilunar cusps, because of the crista supraventricularis, a muscular structure wedged in between and consisting of septal and parietal components. This big structure, hanging over the RV, accounts for the anterior position of the RVOT when compared to the LVOT. The posterior leaflet of the tricuspid valve is attached to the ring of the posterior AV sulcus, from the acute margin to the crux cordis, and delimited by the anterolateral and posteroseptal commissures. Seen from outside, the acute margin of the heart roughly indicates the border between the anterior and posterior RV free walls and anterior and posterior leaflets. It corresponds to the anteroposterior commissure of the tricuspid valve.

The tricuspid valve commissures, defined as the boundary between two leaflets where the distance from the free margin to the AV ring is shorter, show leaflet continuity. However, anteroseptal commissure discontinuity is seen in 20–30% of cases so that the underlying membranous septum appears bare. This facilitates intracavitary recording of His bundle electrical activity as well as ablation to achieve iatrogenic AV block when necessary [38].

Tricuspid valve leaflets exhibit first-order chordae, attached to the free margin, and second-order chordae attached to the ventricular surface (rough zone of the leaflets), anchoring the subvalvular apparatus (so-called strut chordae). Third-order short chordae arise close to the basal attachment of the mural leaflets (anterior and posterior), as seen in the mitral valve.

Right ventricular outflow tract

The outlet part of the RV corresponds to the embryonic "conus" or bulbus cordis, so-called because of its conical shape (Figure 2.4). It starts proximally from the moderator band, a peculiar muscular bundle originally described by Leonardo da Vinci in his outstanding anatomical pictures (Figure 2.5). Leonardo employed the adjective "moderator" due to the alleged function to restrain the action of the anterior papillary muscle of the tricuspid valve, anchoring its base to the ventricular septum. It connects the anterior papillary muscle of the tricuspid valve to the septal band. Together, they are known as the trabecula septomarginalis or septomarginal band. The septal band, namely the septal part of the trabecular septomarginalis, is a prominent, distinct structure of the right-sided surface of the ventricular septum and represents a landmark of the RV (see Figure 2.4). The right bundle branch runs under the subendocardium and, when reaching the moderator band, divides with a distinctive branch coursing along the anterior papillary muscle of the tricuspid valve. The proximal part of the septal band, at the level of the Lancisi (conal) muscle, divides into two limbs, one anterior and one posterior, with a sling configuration, hosting the septal branch of the crista supraventricularis. The anterior wall of the pulmonary infundibulum may show thick trabeculae originating from the ventricular septum (septoparietal bands), different from the parietal band of the crista (see Figure 2.4).

There are three semilunar cusps (anterior, postero-right, and postero-left) within the sinuses of Valsalva and separated by commissures. The cusps are attached to the

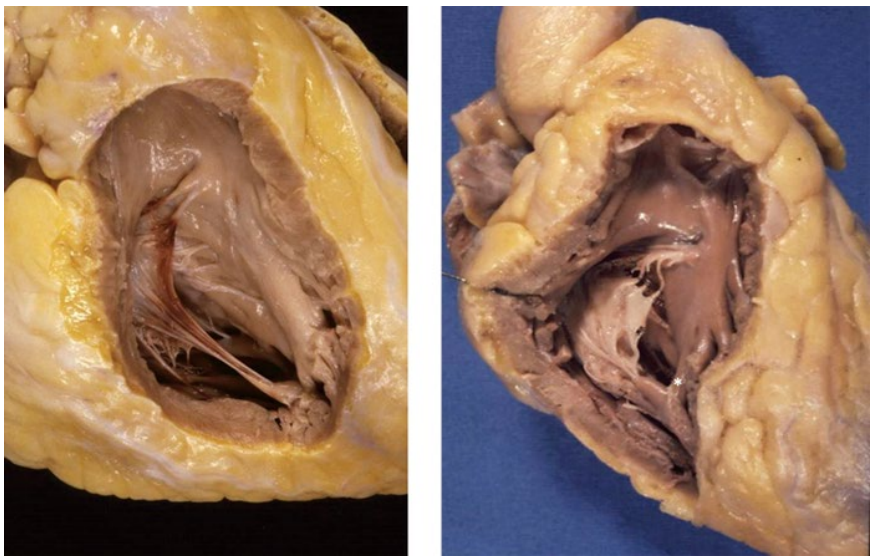

Figure 2.4 The outflow tract of the right ventricle from the moderator band to the pulmonary valve.

(a) (b)

Figure 2.5 (a) Original drawing of the moderator band by Leonardo da Vinci. (b) The same in an ovine heart.

pulmonary wall, which is an essential part of the valve apparatus. Overall, they show a crown-shaped ring and lie over the infundibular myocardium (Figures 2.6, 2.7). The latter regularly extends over the ring, so the myocardium of the RV is located beyond the hemodynamic ventriculoarterial boundary (see Figure 2.7). This explains the apparent paradox of arrhythmias originating from the pulmonary artery. Indeed, the pulmonary root is higher than the aortic root. Thus, the infundibular septum (namely, the septal band of the crista supraventricularis) separates the pulmonary infundibulum from the sinus portion of the aorta, like a ventriculoarterial septum (Figures 2.8, 2.9). Thus, the infundibular septum is within the sinus portion of the aorta, seen from the left side. This may explain "aortic" arrhythmias, originating from the aortic side of the infundibular septum.

The myocardium of the RV free wall is 3–4 mm thick in the normal adult, with a variable amount of fatty tissue infiltrating the subepicardial layer. In obese people, an extensive lipomatous infiltration may be observed ("adipositas cordis"), equivalent to the subcutaneous adipose tissue. This should not be confused with the fibrofatty replacement of arrhythmogenic cardiomyopathy [39].

Anatomy of the left ventricle

The LV is a posterior chamber between the mitral and aortic valves. Seen from the outside with an epicardial view, it may be easily identified on the left side of the heart, between the anterior and posterior descending coronary arteries, which run in the anterior and posterior

interventricular grooves, respectively. The shape of the cavity is oval with inflow and outflow tracts separated by the anterior (aortic) mitral leaflet (Figure 2.10). The LV may be divided into three parts: inlet, apex, and outlet.

The inflow contains the left AV apparatus, which consists of two leaflets, chordae tendinae, and two groups of papillary muscles. The shape of the mitral valve apparatus mimics a bishop's miter, thus explaining why Andreas Vesalius coined the term "mitral." The anterior leaflet is a large curtain receiving chordae from both anterolateral and posteromedial papillary muscles. It is deeper and narrower than the posterior one. It is in fibrous continuity with the aortic valve (all posterior and part of the left coronary cusps), and is not inserted into the AV ring (Figure 2.11). The posterior ("mural") mitral leaflet is larger and less deep than the anterior but the areas of both are almost equal. It is attached to the AV ring, which provides discontinuity between the atrial and ventricular myocardium. The posterior leaflet usually consists of three scallops, separated by commissural-like indentations, known as "cleft commissures," marked by fan cleft-like

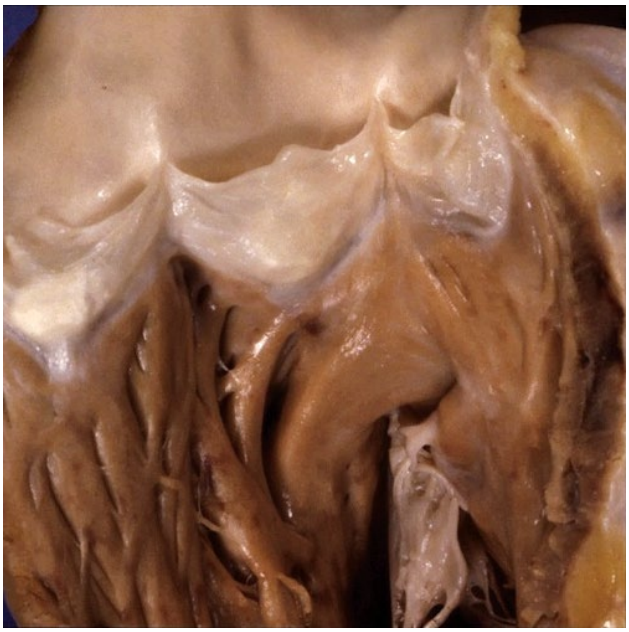

Figure 2.6 Close-up of the pulmonary infundibulum (right ventricular outflow tract). Note the Lancisi muscle: the crista supraventricularis with parietal and septal bands. All of the pulmonary semilunar cusps lie over musculature.

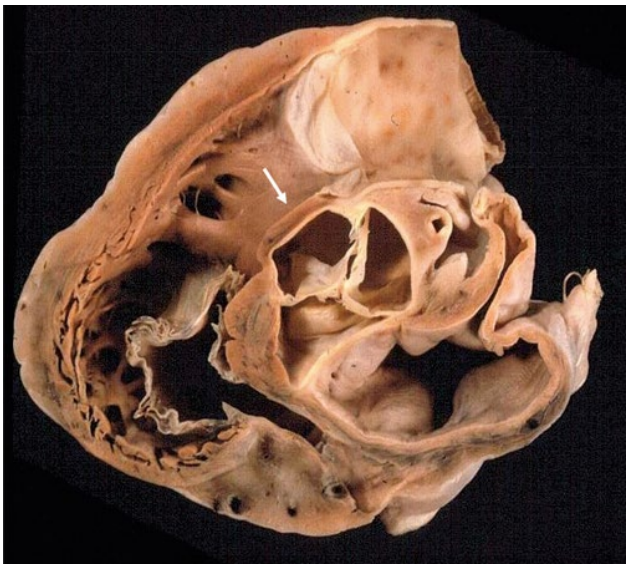

Figure 2.8 Basal short axis section of a cardiac specimen. The right and left outflow tracts are crossing over. Arrow indicates the so-called infundibular septum (septal band of crista supraventricularis) separating the subvalvular pulmonary outflow from the supravalvular right aortic sinus.

Figure 2.7 (a) Pulmonary arterial root: all the cusps are attached to muscle. (b) Histology of the postero-left pulmonary semilunar cusp: the myocardium is well over the basal ring (hemodynamic border between the ventricular and pulmonary artery), and may be the source of "pulmonary" arrhythmias.

(a)

(b)

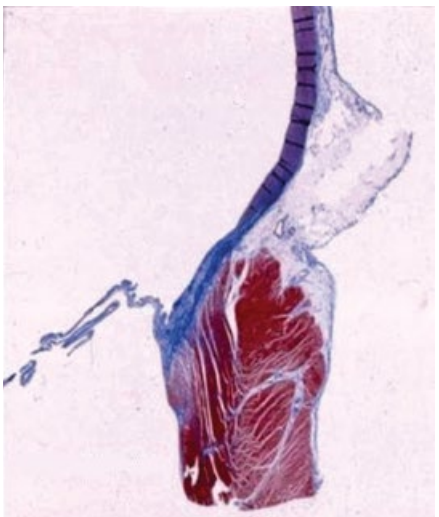

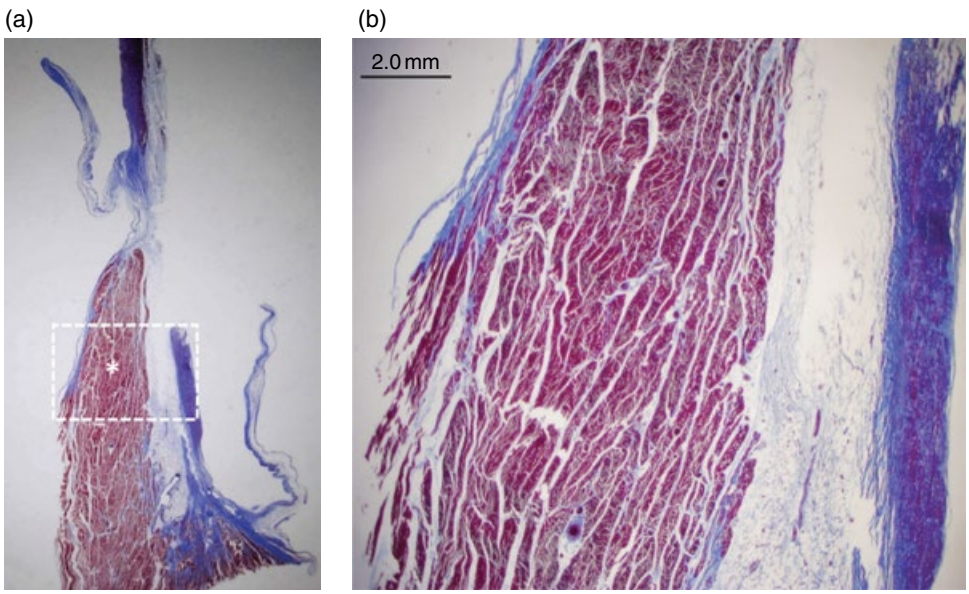

Figure 2.9 (a) Long axis view of the ventricular outflow tract. Asterisk indicates the "infundibular septum" separating the subpulmonary infundibulum from the right aortic sinus. (b) Histology of the "infundibular septum," located just in front of the right aortic sinus. Access for ablating outflow tracts arrhythmias may be through the aorta.

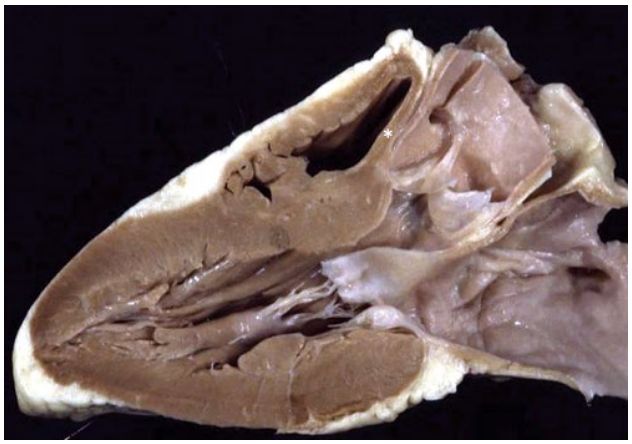

Figure 2.10 Left ventricle in a long axis view. Note the inflow hosting the mitral valve, the apex with thin trabeculations, and the outflow tract corresponding to the smooth basal ventricular septum. Note the anterior (aortic) leaflet of the mitral valve separating the inflow from the outflow tract. The asterisk indicates the "infundibular" septum separating the pulmonary outflow tract from the sinus portion of the aorta.

chordae taking origin from the tips of the posteromedial papillary muscle. The anterolateral papillary muscle, which consists of a single pillar, is different from the posteromedial, which consists of two or more pillars with several tips to support the wider leaflet. The anterolateral and posteromedial commissures represent the boundary between the leaflets, where they approximate each other but still keep in continuity. The commissures are well indicated by fan-like chordae arising from the apex of the

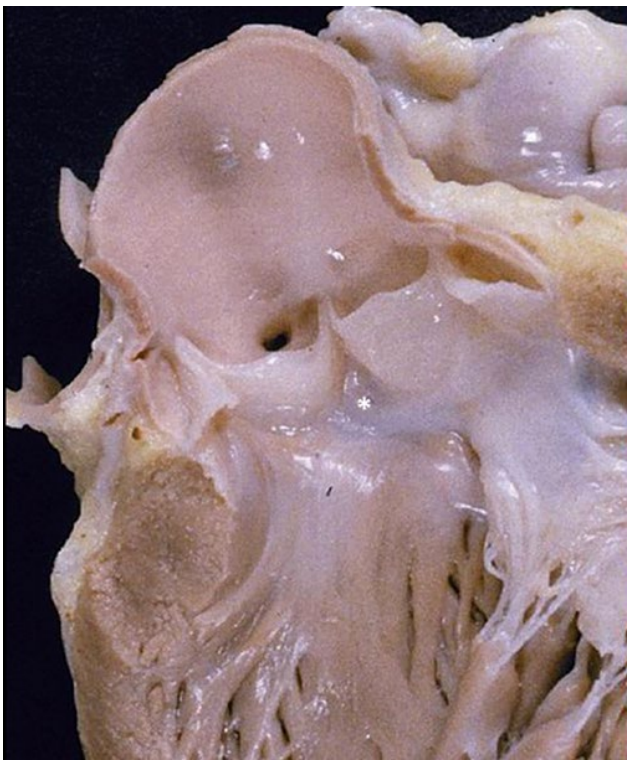

Figure 2.11 The left ventricular outflow tract. Note the mitral valve free from attachment to the ventricular septum, the membranous septum (*) in between the right and non-coronary cusps. The latter and partially the left are in fibrous continuity with the anterior ("aortic") leaflet of the mitral valve. Note the smooth basal part of the ventricular septum.

papillary muscle pillars or tips. The chordae tendinae consist of three orders: the first order is attached to the free margin of the leaflet, the second order is attached to the ventricular surface (rough zone), and the third order arises from the posterolateral free wall (mediated or not by tiny papillary muscles), anchoring the posterior leaflet close to the AV ring. Some of the second-order chordae to the anterior (aortic) leaflet are particularly long and thick and act as strut chordae to sustain the systolic closure of the mitral valve at high pressure.

The apical portion of the LV consists of tiny trabeculae and a thinner wall (see Figure 2.10). It usually forms the apex of the heart, although a bifid apex from both the RV and LV is not a rare occurrence.

The LVOT is posterior and inferior to the RVOT. They cross each other, with the anterosuperior right one running from right to left and the posteroinferior left one running from left to right.

Because of the discontinuity between the tricuspid and pulmonary valves by the crista supraventricularis, the pulmonary root is superior and to the left and the aortic root inferior and to the right.

The LVOT is wedged between the ventricular septum (anterosuperiorly) and the aortic mitral leaflet (posteroinferiorly). Here, the septum is smooth without a septal band. At difference from the RVOT, which starts from the moderator band, it is hard to establish a landmark origin of the LVOT. We might mark it in the border between the smooth and the trabecular parts of the left side of the ventricular septum, which corresponds to the free margin of the anterior (aortic) mitral leaflet in diastole. The length of the LVOT varies according to the cardiac phases. It is long and tubular during diastole at the opening of the anterior (aortic) mitral leaflet and much shorter during systole, when the anterior leaflet moves posteroinferiorly to close the mitral orifice and stick with the posterior leaflet. No muscular structure, such as the crista supraventricularis of the RV, is interposed in between the aorta and the mitral valve (see Figure 2.11). An anterolateral muscle band, variable in thickness, is located between the ventricular septum and the anterior leaflet of the mitral valve, just underneath the left coronary cusp.

The aortic valve apparatus is housed within the sinus portion of the ascending aorta (sinuses of Valsalva). The aortic valve is tricuspid (see Figure 2.11) and consists of:

- a posterior, non-coronary sigmoid cusp, which is in fibrous continuity with the anterior (aortic) leaflet of the mitral valve
- a left coronary cusp, in continuity with both the anterior mitral leaflet and the anterolateral muscle band
- an anterior right coronary cusp, lying over the myocardium of the ventricular septum.

Compared to the pulmonary valve, which is entirely over the myocardium of the pulmonary infundibulum, the aortic valve attaches either to the septal and anterolateral myocardium or to fibrous tissue of the aortic-mitral continuity (Figure 2.12). The aortic ring is crown-shaped with intercuspal triangles, their apex representing the commissures, namely the highest attachment of the cusps to the aortic wall (see Figure 2.11).

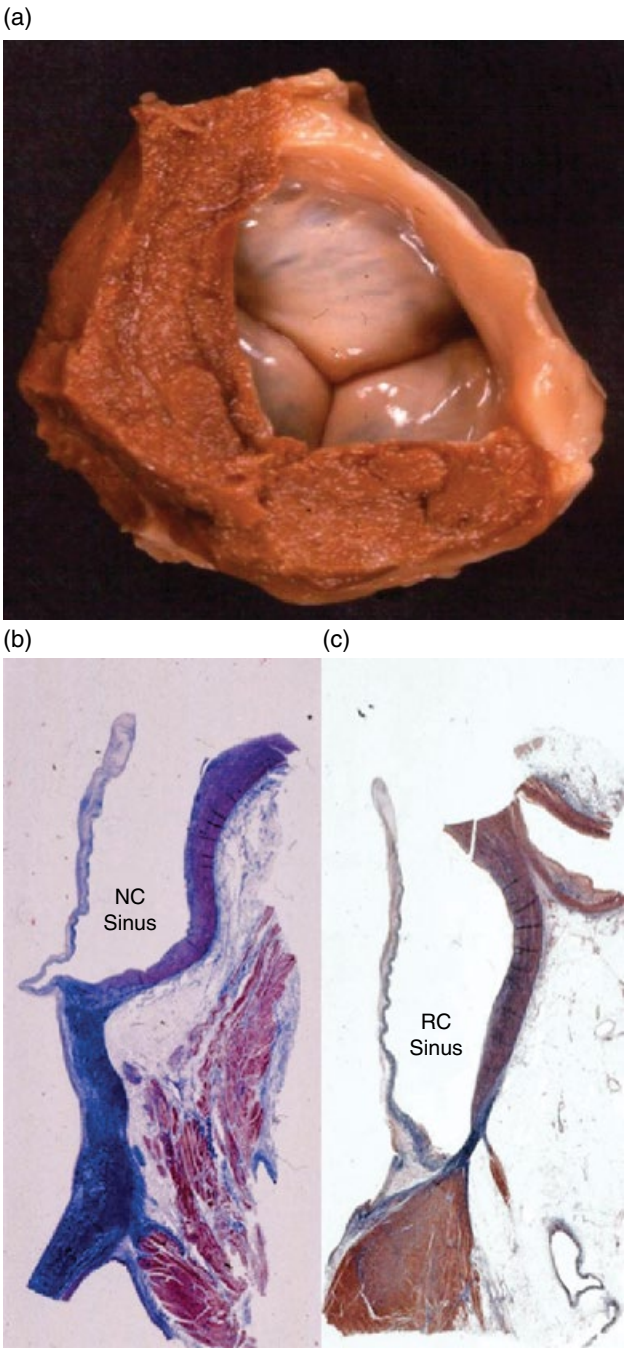

Figure 2.12 (a) Aortic root: the whole non-coronary cusp and part of the left coronary cusp are in fibrous continuity with the mitral valve, whereas the entire right coronary and part of the left coronary cusp are attached to muscle. (b) Histology of the mitro-aortic fibrous continuity. (c) Histology of the right coronary sinus with ventricular septal myocardium over the valve ring. NC, non-coronary; RC, right coronary.

Compared to the mitral valve leaflets, which are still in continuity at the commissures, both the pulmonary and aortic semilunar cusps are in discontinuity at the commissural level.

Atrioventricular conduction system and ventricular outflow tracts

The axis of the AV conduction, the specialized structure joining the atria to the ventricles, is topographically related on the right side to the inflow and on the left side to the outflow [38]. The AV node is located on the right side of the atrial septum within the so-called triangle of Koch, in front of the opening of the coronary sinus. The His bundle penetrates the central fibrous ring at the apex of the Koch triangle and runs underneath the membranous septum over the crest (or on the left) of the ventricular septum, and then divides into right and left bundle branches. The right bundle branch at the level of the Lancisi (conal) septum turns down with either a subendocardial or, more frequently, an intramyocardial course. The left bundle branch spreads out like a sheet in the subendocardium of the left side of the ventricular septum, subdividing into anterior and posterior fascicles. Because of the crista supraventricularis, the His bundle is not exposed to the RVOT whereas it is an intrinsic part of the LVOT. When seen from above (aorta), the commissure in between the non-coronary and right aortic cusps is a landmark, being located just above the His bundle. The distance between the aortic surgical ring (the so-called cusp "nadir") and the His bundle in the adult is about 3–5 mm (Figure 2.13).

Pathology of non-ischemic arrhythmias from the ventricular outflow tract

Most of the tachyarrhythmias arising from the ventricular outflow have a substrate, accounting for triggered activity or reentry circuits, and are mostly non-ischemic. More rarely, the culprits are merely functional disorders, including ion channel diseases. Differential diagnosis between the two entities (organic versus functional) may be pursued *in vivo* with the help of tissue characterization imaging tools and endomyocardial biopsy, which still remains the gold standard in some patients. The latter tool is in fact able to detect histological or ultrastructural abnormalities like inflammation, fibrosis, necrosis or adipose tissue, storage disease or infiltrative interstitial deposits.

(a)

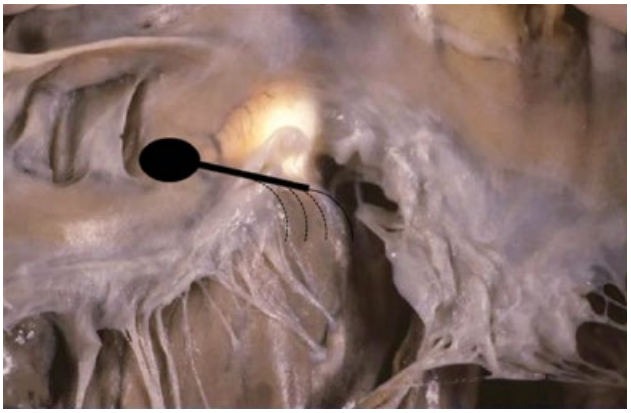

(b)

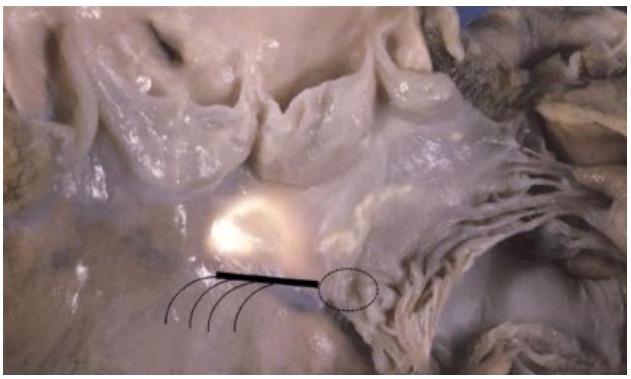

Figure 2.13 The AV conduction system, which is mostly exposed to the left ventricular outflow tract, in a tight relationship with the membranous septum. (a) View from the right side. (b) View from the left side.

Non-ischemic arrhythmic substrates of the RVOT

Arrhythmogenic cardiomyopathy

Arrhythmogenic cardiomyopathy is heredo-familial disorder due to mutations of genes encoding cell junction proteins (desmosome), characterized by a pathognomonic substrate, namely fibro-fatty replacement of the ventricular myocardium (Figures 2.14, 2.15) [40–43].

Originally believed to be confined to the RV and featured by ventricular arrhythmias with left bundle branch morphology, it has been recently recognized as biventricular cardiomyopathy or even involving only the LV with isolated non-ischemic scars and polymorphic ventricular arrhythmias. Nowadays, the original term arrhythmogenic RV cardiomyopathy has been replaced with arrhythmogenic cardiomyopathy.

Ventricular electrical instability is high, which explains the propensity to sustained ventricular tachycardia/fibrillation with cardiac arrest, mostly occurring during effort. It has been well demonstrated, in both human and animal models, that it is a genetically determined

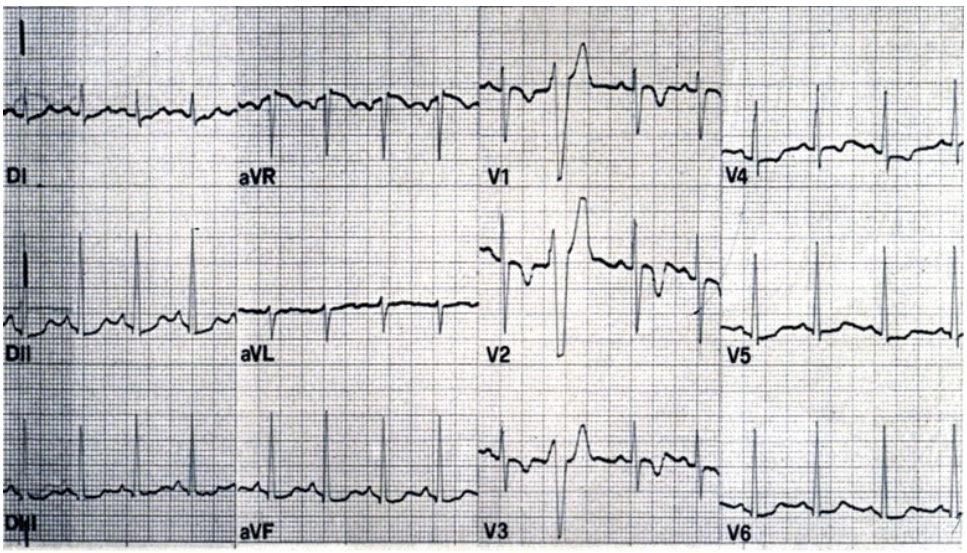

Figure 2.14 Arrhythmogenic cardiomyopathy with fibro-fatty replacement of the right ventricular outflow tract. The ECG shows inverted T waves in the precordial leads and an apparently innocent premature ventricular beat.

cardiomyopathy, with onset and progression of myocyte death and fibro-fatty replacement occurring during childhood, adolescence, and adulthood. Since loss of the myocardium begins after birth, arrhythmogenic cardiomyopathy cannot be considered a congenital heart disease (defect present at birth). The phenomenon of cell death, with fibro-fatty replacement as a consequence of repair, starts from the epicardium. In the RV it extends progressively deeper into the endocardium like a wave front phenomenon, so it is reachable by the bioptome at

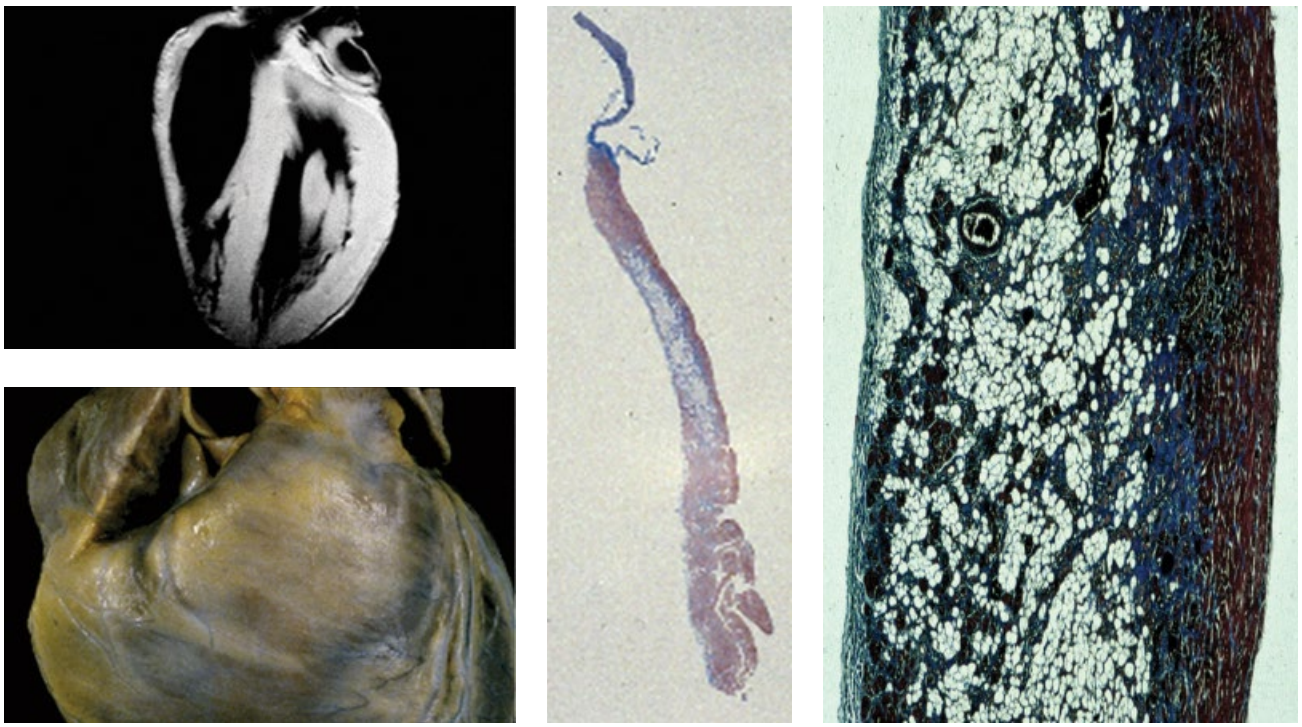

Figure 2.15 Segmental arrhythmogenic cardiomyopathy with fibro-fatty replacement limited to the pulmonary infundibulum (postmortem CMR, gross view, panoramic and close-up histology of the RVOT).

endomyocardial biopsy. When transmurally replaced by fibro-fatty tissue, the RV wall becomes thin and weak, leading to remodeling with the development of ventricular aneurysms in the so-called triangle of dysplasia (inflow, apex, outflow). The RV cavity becomes enlarged with depressed contractility and decreased ejection fraction. RVOT dilation is a common occurrence, easily seen by echocardiography. The aneurysm located at the inflow in the subtricuspid diaphragmatic wall should be considered a pathognomonic marker of arrhythmogenic cardiomyopathy.

The RV remodeling explains the typical phenotype of this cardiomyopathy.

- Electrical disorders consisting of delayed ventricular depolarization (large QRS, epsilon wave, late potentials), repolarization abnormalities (inverted T waves in right precordial leads exploring the outlet and anterior wall of the RV), ventricular tachyarrhythmias with left bundle branch block morphology, positive electrophysiological test at ventricular stimulation. The aneurysms favor reentry circuits of the electrical stimulus with onset of ventricular arrhythmias.
- Depressed ventricular contractility, which may lead to congestive heart failure. In advanced stages, it may be so severe that it may require cardiac transplantation. Arrhythmogenic cardiomyopathy, mimicking dilated cardiomyopathy, accounts for 4% of indications of cardiac transplantation [44]. RV enlargement, aneurysms and depressed contractility are well visible by two-dimensional echocardiography, which represents a low-cost, rapid tool for assessment of ventricular remodeling and dysfunction. Contrast cardiac magnetic resonance imaging, with late enhancement by gadolinium, adds information on tissue composition by visualizing fibro-fatty replacement [45].
- In 80% of cases of fibro-fatty infiltration, the phenomenon is topographically diffused with the occurrence of aneurysms [41]. Oddly enough, the ventricular septum is almost always spared and cannot be considered the target for endomyocardial biopsy as a source of fibro-fatty tissue. The RV disease may be segmental, with sole involvement of the RVOT, as a source of infundibular tachyarrhythmias and may require differential diagnosis with idiopathic RVOT tachycardia (Figures 2.17, 2.18). The pathology of the LV in arrhythmogenic cardiomyopathy includes "non-ischemic scars," typically located in the subepicardium – midwall. Since the disease is biventricular in 70% of cases, and the LV "scars" are easily detectable by cardiac magnetic resonance, the LV may be considered the diagnostic "mirror" of the RV in arrhythmogenic cardiomyopathy [45].
- "Electrical" scars, namely myocardial areas that are electrically silent at electroanatomical mapping. No electrical activity may originate from areas with

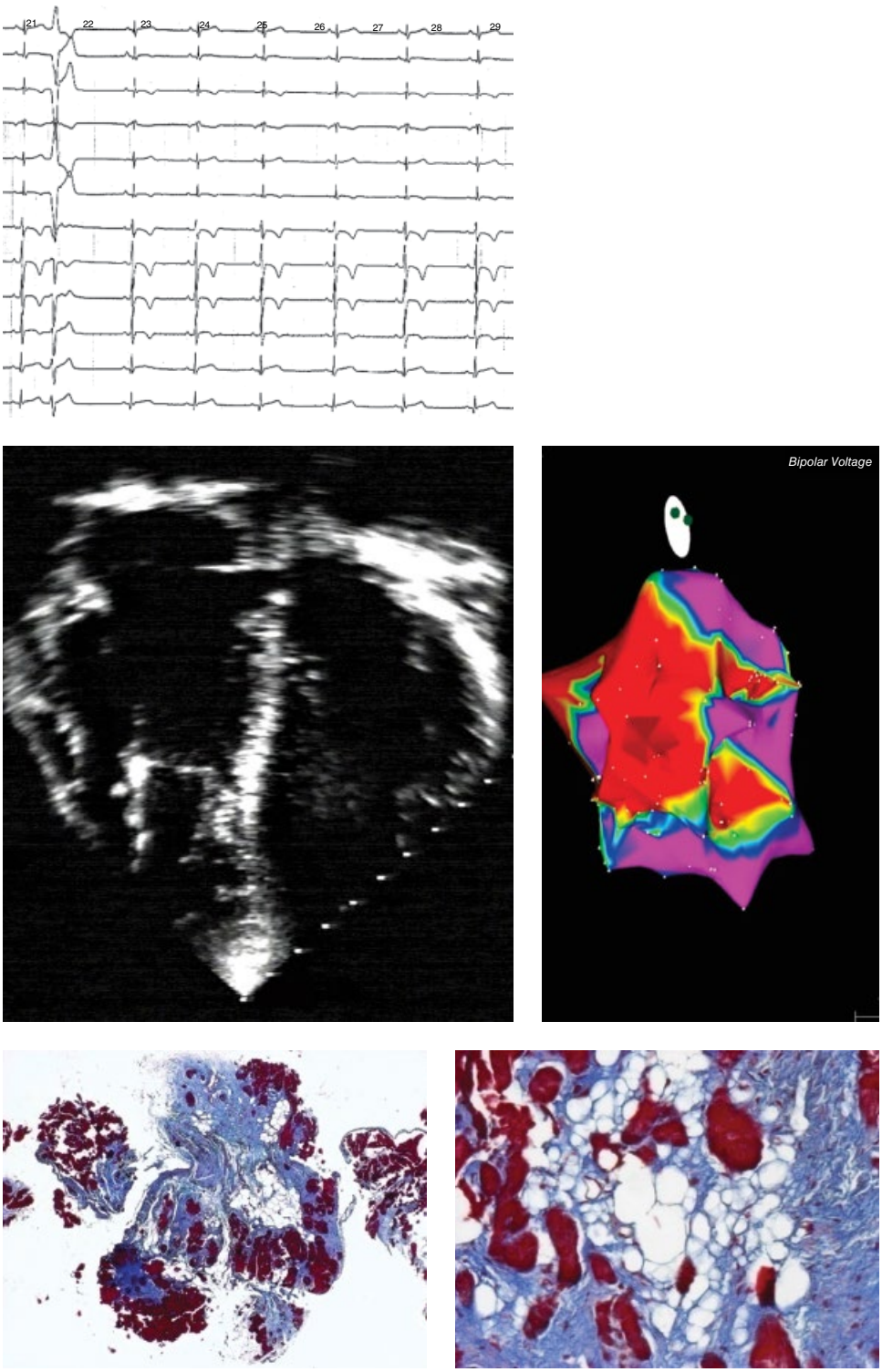

Figure 2.16 Electrophysiological mapping of extensive electrical scars and an endomyocardial biopsy showing severe fibro-fatty replacement in a patient with ECG and echocardiographic features of arrhythmogenic cardiomyopathy.

fibro-fatty replacement (see Figures 2.16, 2.17, 2.18) [45,46]. It is interesting to note that, as far as the RV free wall, because of the pathological thinning, electro-anatomical mapping is superior to contrast cardiac magnetic resonance to visualize areas of "non-ischemic" fibro-fatty scars.

- Right ventricular endomyocardial biopsy plays a pivotal role in the *in vivo* diagnosis by detecting the substrate

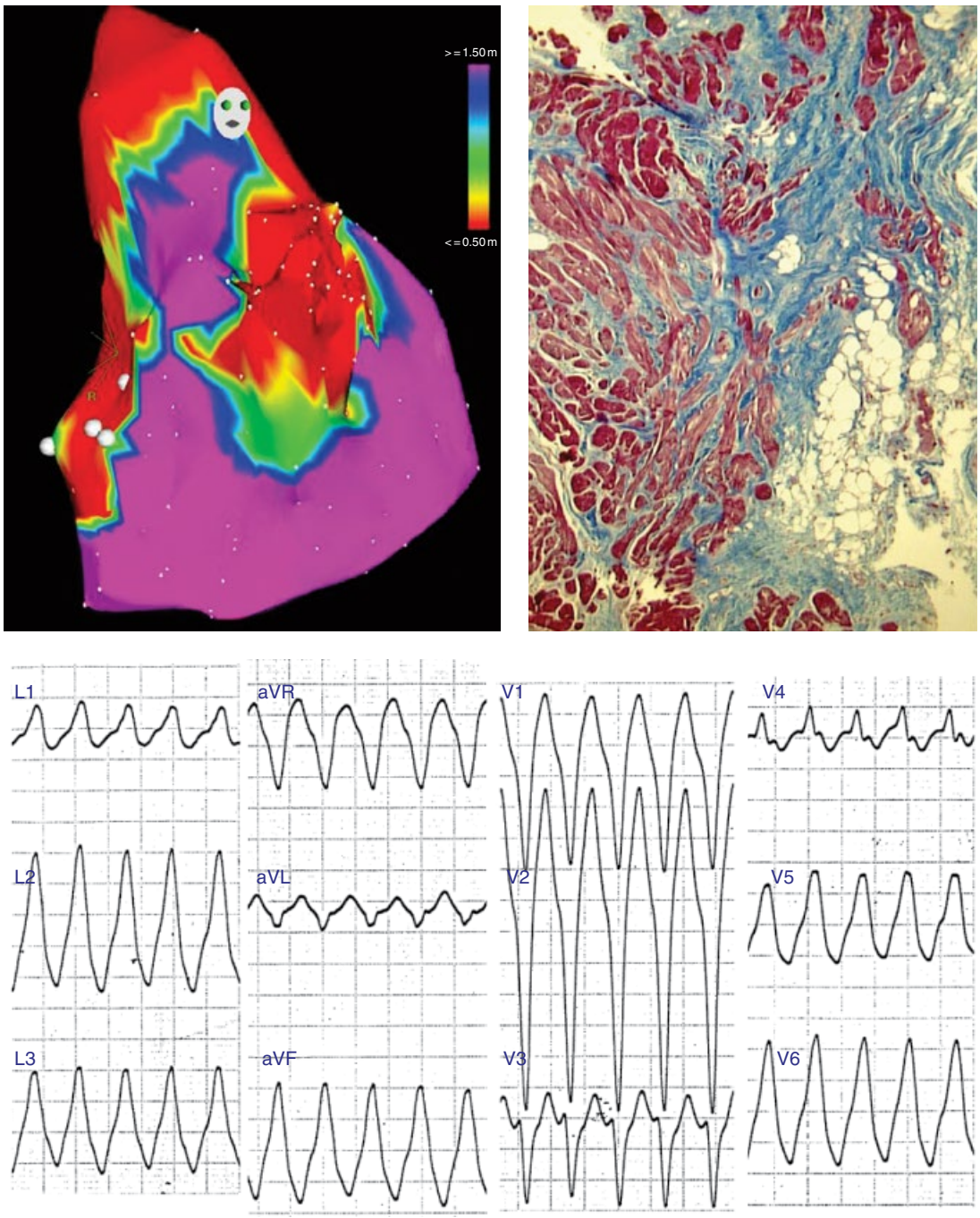

Figure 2.17 Electrophysiological mapping showing infundibular electrical scars and an endomyocardial biopsy with fibro-fatty replacement. The ECG shows left bundle branch block ventricular tachycardia with inferior axis.

of fibro-fatty replacement. Histomorphometric quantitative parameters have been calculated, thus providing major and minor criteria for the tissue characterization category [47,48]. When the residual myocardium (which accounts for 85% of the area in the normal heart) is less than 60% in a bioptic sample due to fibro-fatty replacement, the histological examination is pathognomonic for arrhythmogenic cardiomyopathy and is nowadays considered one of the major criteria for achieving the final diagnosis (see Figures 2.16, 2.17). To increase the sensitivity, the bioptome should point to the free wall where the fibro-fatty replacement

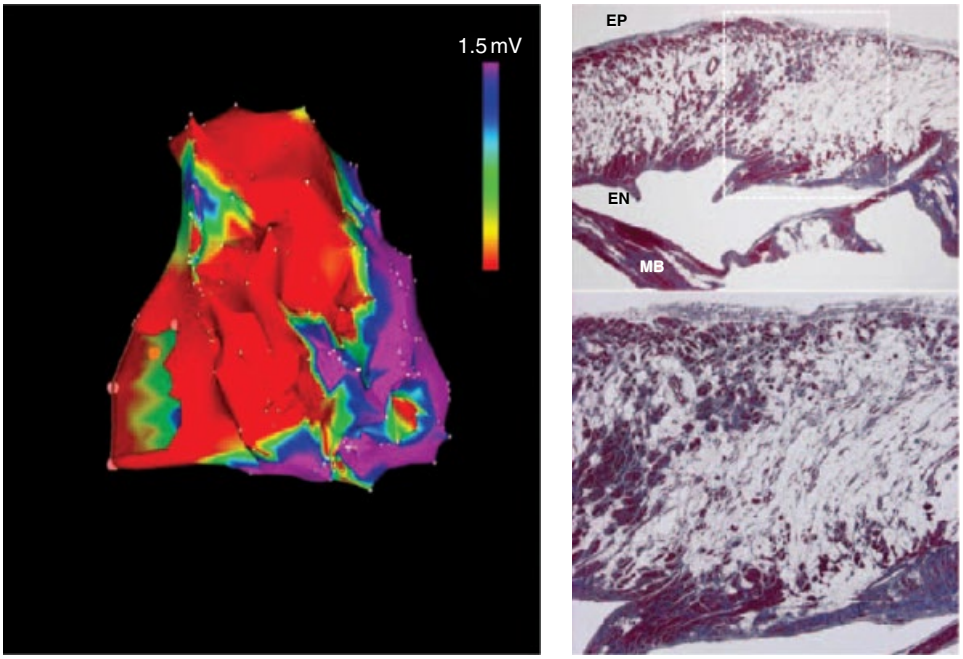

Figure 2.18 Extensive electrical scar by electroanatomical mapping and transmural fibro-fatty replacement of the pulmonary infundibulum at postmortem histology. EP, epicardium; EN, endocardium; MB, moderator band.

may be transmural, reaching the endocardium, and not the ventricular septum which is exceptionally involved. Perforation is rare and the risk is acceptable since it is not life-threatening and cardiac tamponade remains exceptional. However, bleeding may occur although rarely. Immunostaining for plakoglobin has been proposed as an additional diagnostic marker of arrhythmogenic cardiomyopathy [49], but additional validation is required.

Myocarditis

Ventricular arrhythmias are one of the clinical presentations of myocarditis, especially when focal without impairment of contractility and congestive heart failure [50]. Acute myocarditis may be localized in the RVOT and be the origin of ventricular arrhythmias with left bundle branch block morphology [51]. Lymphocyte infiltrates associated with myocyte death and inflammatory edema may interfere with Na + or K+ inflow-outflow and myocyte depolarization-repolarization, thus accounting for electrical instability.

Endomyocardial biopsy is still the gold standard for diagnosis, even though in cases of focal myocarditis the sampling error may be high. Several pieces of endomyocardium are mandatory to avoid sampling errors and increased sensitivity. Molecular investigation with polymerase chain reaction in acute early phase may help to establish the precise etiological diagnosis, whether RNA (especially enterovirus) or DNA (especially adenovirus) viruses. It is interesting to note that myocarditis in the acute phase may not be associated with extensive loss of myocardium so that electroanatomical mapping may produce negative results. In this setting, the coupling of electroanatomical mapping and endomyocardial biopsy plays a key role in differential diagnosis between arrhythmogenic cardiomyopathy (electroanatomical mapping and biopsy both positive because of fibro-fatty replacement) and myocarditis (electroanatomical mapping negative and endomyocardial biopsy positive) (Figure 2.19), as well as idiopathic tachycardia of the RVOT (electroanatomical mapping and endomyocardial biopsy both negative) [51,52] (Figure 2.20).

Sarcoidosis

Clinically evident cardiac involvement may occur in 5% of patients with sarcoidosis, even as a primary manifestation [53]. Another 20–25% of pulmonary/systemic sarcoidosis patients have asymptomatic cardiac involvement (clinically silent disease). Although conduction disturbances and heart failure are the main clinical signs, ventricular arrhythmias are also a common presentation.

The disease is mostly a multisystem, non-infective, granulomatous morbid entity, with non-caseating granulomas as a pathological hallmark. No specific pattern of

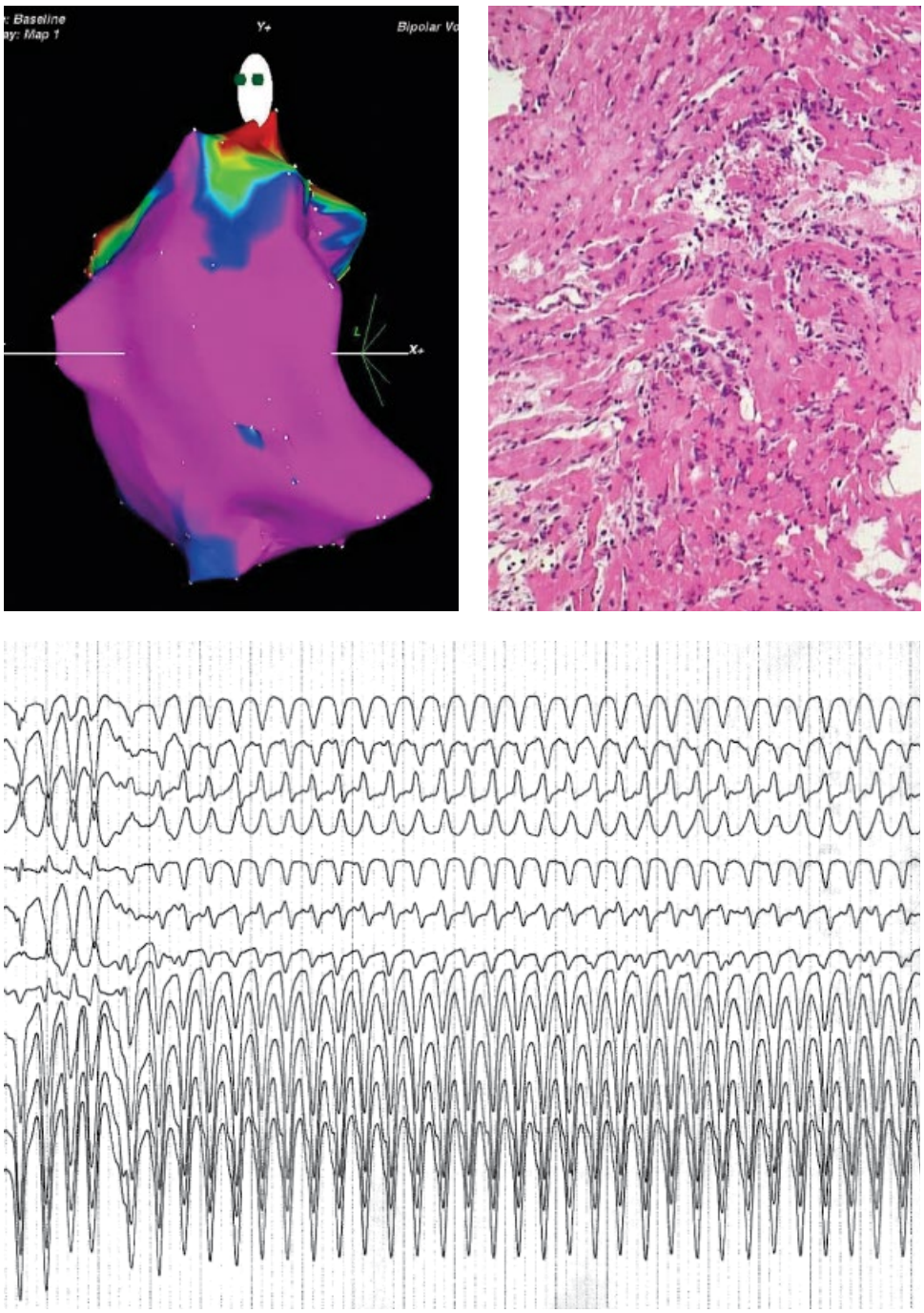

Figure 2.19 Negative electroanatomical mapping and acute myocarditis from an endomyocardial biopsy in a patient with ventricular tachycardia of left bundle branch morphology.

late enhancement is diagnostic for cardiac involvement, although it is most often seen in basal segments (particularly of the septum and lateral wall). By fluorodeoxyglucose positron emission tomography (PET), focal or diffuse fluorodeoxyglucose uptake patterns suggest active cardiac sarcoidosis. Differential diagnosis with other diseases (myocarditis, arrhythmogenic cardiomyopathy) is achieved by endomyocardial biopsy (Figure 2.21) [54,55]. Unfortunately, the sensitivity of biopsy is low (nearly 25%), due to sampling error because the focal nature of the disease. To increase the sensitivity, imaging-guided (PET-cardiac magnetic

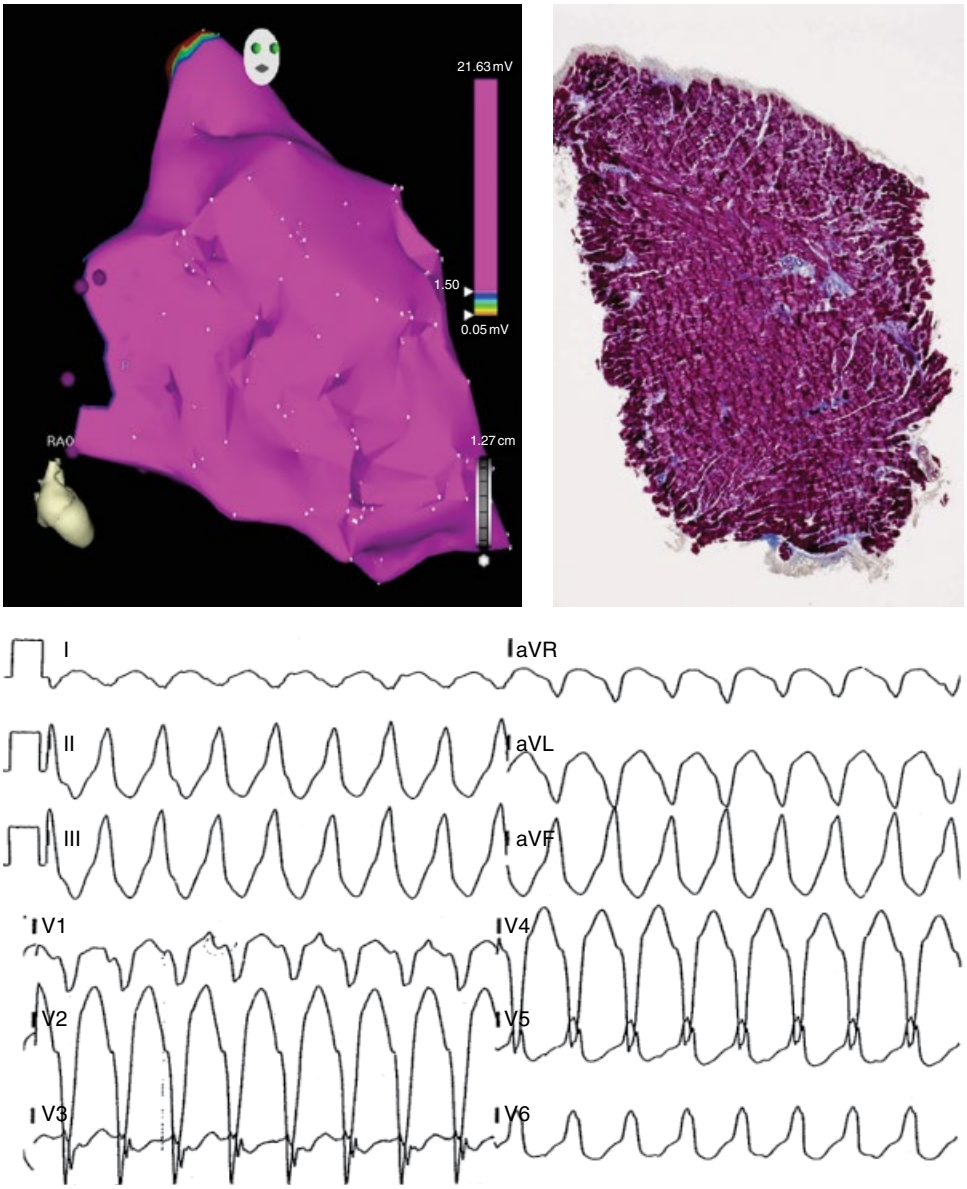

Figure 2.20 Normal electrical activity (negative electrophysiological mapping) and endomyocardial biopsy (preserved myocardium) in a patient with left bundle branch block ventricular tachycardia (idiopathic RVOT tachycardia).

resonance (CMR)) biopsy procedures, especially of the lymph nodes, are recommended and may increase sensitivity up to 50%. In cardiac sarcoidosis, electro-anatomical mapping is positive but non-specific. Thus, endomyocardial biopsy is pathognomonic and still the gold standard for a certain diagnosis of cardiac sarcoidosis.

RVOT ventricular arrhythmias without substrate

RVOT or LVOT tachyarrhythmias (premature ventricular beats, non-sustained and sustained monomorphic ventricular tachycardia, ventricular fibrillation) may occur in the absence of structural myocardial disease. They may originate from either the subvalvular or supravalvular regions in the ventricular outflows. They include myocardium located within the sinus of Valsalva beyond the hemodynamical border of the crown-shaped valve ring of both the pulmonary and aortic semilunar valves [56]. Outflow tract arrhythmias are identified by an electrocardiographic pattern consistent with a left bundle branch block morphology with inferior axis. They are caused by cAMP-mediated triggered activity and terminated by administration of adenosine. They are benign and not genetically determined. Of course, being ventricular arrhythmias without

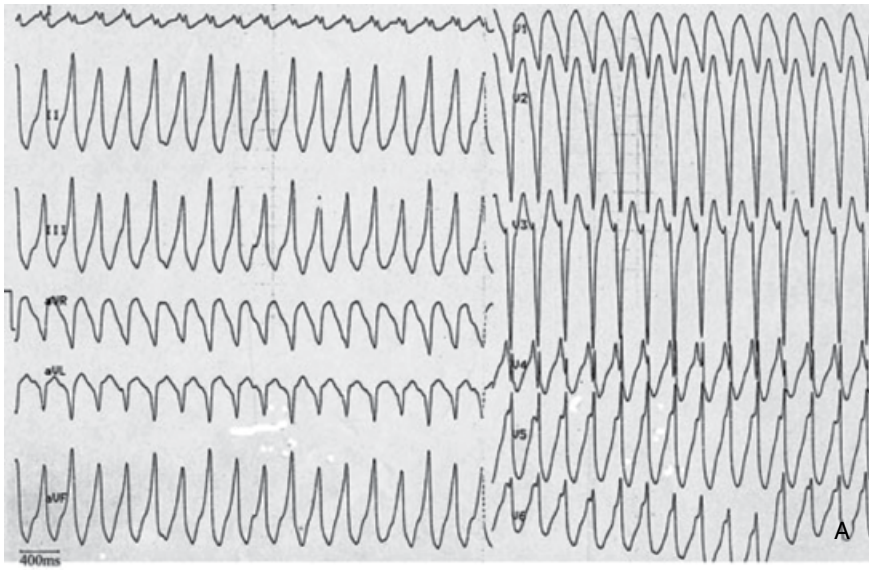

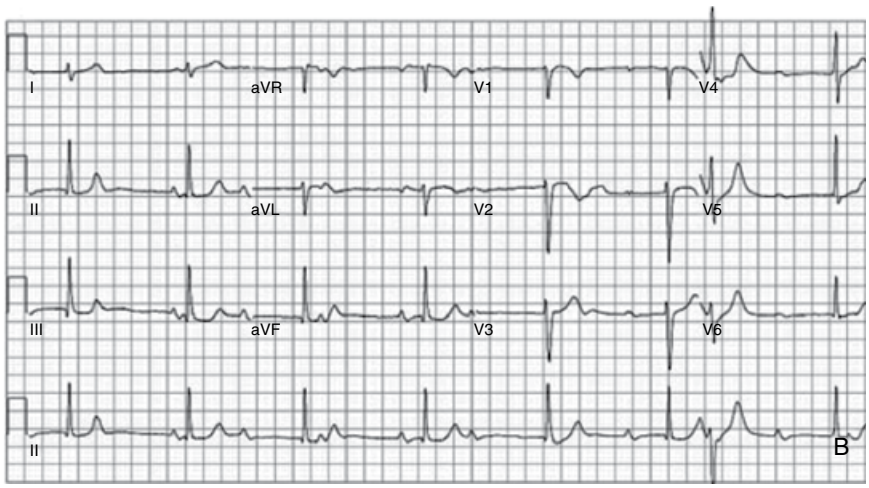

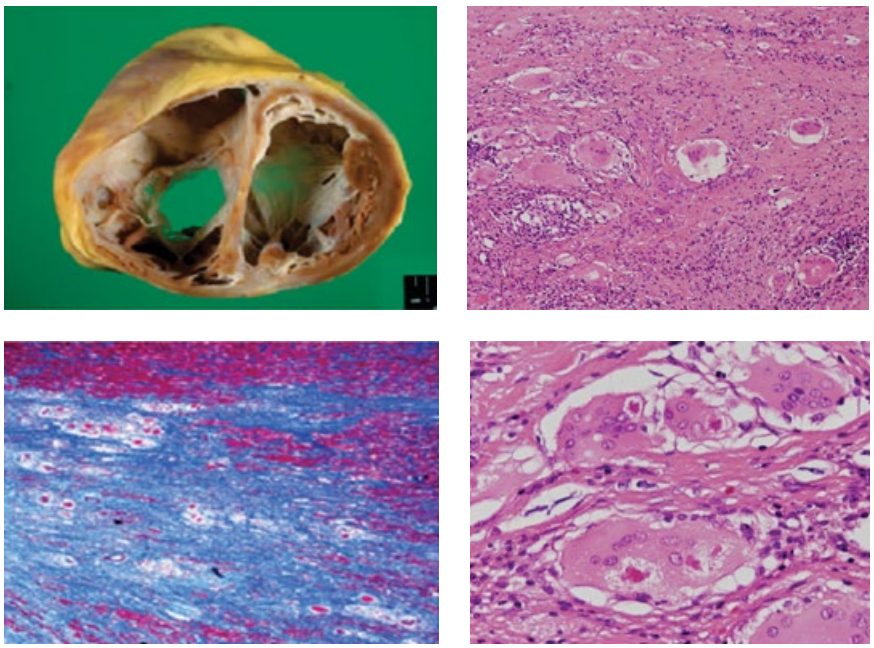

Figure 2.21 Ventricular tachycardia with left bundle branch morphology in a patient with an ECG-clinical diagnosis of arrhythmogenic cardiomyopathy and sarcoidosis identified in the explanted heart at transplantation. Note the non-caseous granuloma.

substrate, unipolar or bipolar electroanatomical mapping results are negative (Figure 2.20). Nonetheless, catheter-based radiofrequency ablation may represent definitive treatment [57].

Brugada syndrome

This is an inherited arrhythmic disorder featuring a non-ischemic ST segment elevation in right precordial leads in a 12-lead ECG [22–25] (Figure 2.22). Mutations of the *SCN5A* gene have been found in about 20% of cases. While the report by the Brugada brothers described a syndrome in survivors of cardiac arrest without structural disease [22], the original description in the literature was of "ventricular fibrillation without apparent heart disease." In fact, structural abnormalities of the RV determined by either autopsy or endomyocardial biopsy were found in five out of six patients [23]. Since then, the presence of a substrate has remained a matter of debate in the literature.

There are two main theories to explain the pathogenesis of Brugada syndrome: repolarization and depolarization. Yan and Antzelevitch first advanced the theory of an abnormal transmural repolarization in the RVOT due to heterogeneous loss of the cardiomyocyte action potential dome in the epicardium [58]. The most compelling evidence in support of the depolarization hypothesis comes from the studies by Nademanee [25,33]. In particular, myocardial fibrosis has been suggested by abnormal, low-voltage,

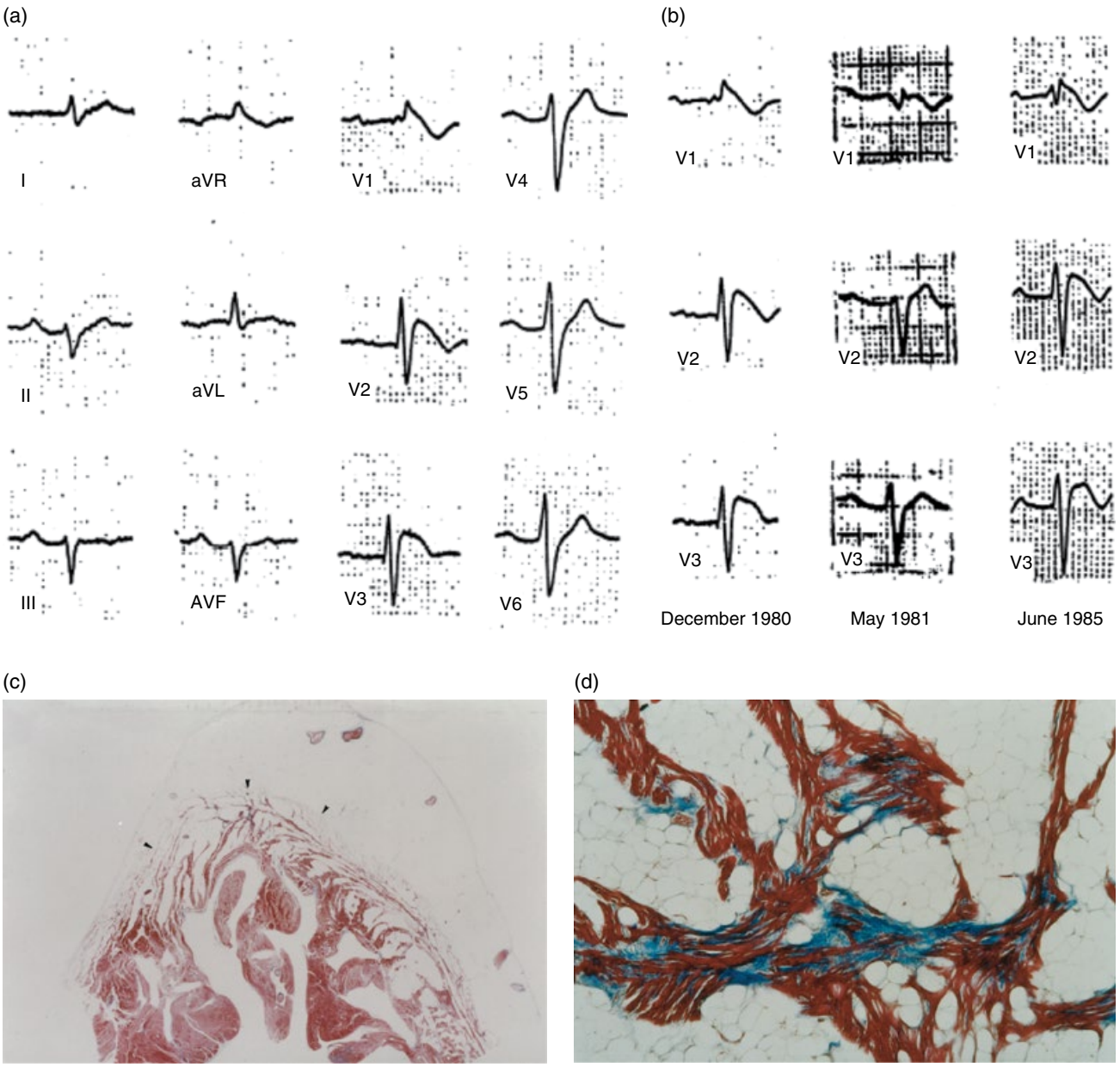

Figure 2.22 Fatty infiltration with mild fibrosis of the right ventricle in a patient with an *in vivo* diagnosis of ST segment elevation, right bundle branch, prolonged PQ interval, and aborted sudden death.

fractionated electrograms localized to the RVOT at the epicardium. The recent description of increased fibrosis, as well as reduced gap junction signaling protein Cx43 in the RVOT in a series of sudden death cases with family history of Brugada syndrome and without evident structural disease, is in favor of the depolarization hypothesis. Furthermore, electrophysiological and imaging studies have identified subtle structural abnormalities in the RVOT of affected patients [29,59,60]. Elimination of the sites of slow conduction gives the rationale for the efficacy of ablation therapy [61,62]. However, Szel et al. provided an alternative cellular electrophysiological mechanism as the basis for late potentials and fractionated electrogram activity in Brugada syndrome, demonstrating that the ECG abnormalities are due to repolarization and not to depolarization defects [63]. Future studies in genotyped cases should address the roles of fibrosis and gap junction proteins in Brugada syndrome.

Although repolarization and depolarization theories may indeed be synergistic and not mutually exclusive, correct assessment of the cellular pathophysiology remains a main target for appropriate therapy. It is important to note that AV conduction disturbances are a common finding in Brugada syndrome (PR prolongation, right bundle branch block). This is not surprising, considering that familial AV block has been explained by mutation of *SCN5A* [64]. Again, whether conduction disturbances are the result of merely functional changes or structural abnormalities of the specialized myocardium (Figure 2.22) remains to be addressed [65,66].

References

1 Chugh SS, Reinier K, Teodorescu C, *et al.* Epidemiology of sudden cardiac death: clinical and research implications. *Prog Cardiovasc Dis.* 2008;**51**:213–28.

2 Huikuri HV, Castellanos A, Myerburg RJ. Sudden death due to cardiac arrhythmias. *N Engl J Med* 2001;**345**:1473–82.

3 Morita H, Fukushima-Kusano K, Nagase S, *et al.* Site-specific arrhythmogenesis in patients with Brugada syndrome. *J Cardiovasc Electrophysiol* 2003;**14**:373–9.

4 Shimizu W. Arrhythmias originating from the right ventricular outflow tract: how to distinguish "malignant" from "benign"? *Heart Rhythm* 2009;**6**:1507–11.

5 de la Cruz MV, Sanchez GC, Arteaga MM, Arguello C. Experimental study of the development of the truncus and the conus in the chick embryo. *J Anat* 1977;**123**:661–86.

6 de Jong F, Opthof T, Wilde AA, *et al.* Persisting zones of slow impulse conduction in developing chicken hearts. *Circ Res* 1992;**71**:240–50.

7 Buckingham M, Meilhac S, Zaffran S. Building the mammalian heart from two sources of myocardial cells. *Nat Rev Genet* 2005;**6**:826–35.

8 Boukens BJ, Christoffels VM, Coronel R, Moorman AF. Developmental basis for electrophysiological heterogeneity in the ventricular and outflow tract myocardium as a substrate for life-threatening ventricular arrhythmias. *Circ Res* 2009;**104**:19–31.

9 Moorman AF, Christoffels VM. Cardiac chamber formation: development, genes, and evolution. *Physiol Rev* 2003;**83**:1223–67.

10 Kelly RG, Brown NA, Buckingham ME. The arterial pole of the mouse heart forms from Fgf10-expressing cells in pharyngeal mesoderm. *Dev Cell* 2001;**1**:435–40.

11 Rana MS, Horsten NC, Tesink-Taekema S, Lamers WH, Moorman AF, van den Hoff MJ. Trabeculated right ventricular free wall in the chicken heart forms by ventricularization of the myocardium initially forming the outflow tract. *Circ Res* 2007;**100**:1000–7.

12 Sizarov A, Lamers WH, Mohun TJ, Brown NA, Anderson RH, Moorman AF. Three-dimensional and molecular analysis of the arterial pole of the developing human heart. *J Anat* 2012;**220**:336–49.

13 Lamers WH, Moorman AF. Cardiac septation: a late contribution of the embryonic primary myocardium to heart morphogenesis. *Circ Res* 2002;**91**:93–103.

14 Theveniau-Ruissy M, Dandonneau M, Mesbah K, *et al.* The del22q11.2 candidate gene Tbx1 controls regional outflow tract identity and coronary artery patterning. *Circ Res* 2008;**103**:142–8.

15 Boukens BJ, Sylva M, de Gier–de Vries C, *et al.* Reduced sodium channel function unmasks residual embryonic slow conduction in the adult right ventricular outflow tract. *Circ Res* 2013;**113**:137–41.

16 Sizarov A, Devalla HD, Anderson RH, Passier R, Christoffels VM, Moorman AF. Molecular analysis of patterning of conduction tissues in the developing human heart. *Circ Arrhythm Electrophysiol* 2011;**4**:532–42.

17 Fijnvandraat AC, van Ginneken AC, de Boer PA, *et al.* Cardiomyocytes derived from embryonic stem cells resemble cardiomyocytes of the embryonic heart tube. *Cardiovasc Res* 2003;**58**:399–409.

18 Sadauskas VM, Mutskus KS, Puodzhius SS, Bukauskas FF. Electrical activity of human embryo heart cells under hypoxic conditions. *Akush Ginekol (Mosk)* 1976:19–22.

19 Dobrzynski H, Anderson RH, Atkinson A, *et al.* Structure, function and clinical relevance of the cardiac conduction system, including the atrioventricular ring

and outflow tract tissues. *Pharmacol Ther* 2013;**139**:260–88.
20 Christoffels VM, Moorman AF. Development of the cardiac conduction system: why are some regions of the heart more arrhythmogenic than others? *Circ Arrhythm Electrophysiol* 2009;**2**:195–207.
21 Kleber AG, Rudy Y. Basic mechanisms of cardiac impulse propagation and associated arrhythmias. *Physiol Rev* 2004;**84**:431–88.
22 Brugada P, Brugada J. Right bundle branch block, persistent ST segment elevation and sudden cardiac death: a distinct clinical and electrocardiographic syndrome. A multicenter report. *J Am Coll Cardiol* 1992;**20**:1391–6.
23 Martini B, Nava A, Thiene G, *et al.* Ventricular fibrillation without apparent heart disease: description of six cases. *Am Heart J* 1989;**118**:1203–9.
24 Antzelevitch C, Brugada P, Borggrefe M, *et al.* Brugada syndrome: report of the second consensus conference. *Heart Rhythm* 2005;**2**:429–40.
25 Nademanee K, Veerakul G, Chandanamattha P, *et al.* Prevention of ventricular fibrillation episodes in Brugada syndrome by catheter ablation over the anterior right ventricular outflow tract epicardium. *Circulation* 2011;**123**:1270–9.
26 Chen Q, Kirsch GE, Zhang D, *et al.* Genetic basis and molecular mechanism for idiopathic ventricular fibrillation. *Nature* 1998;**392**:293–6.
26a Kyndt F, Probst V, Potet F, *et al.* Novel SCN5A mutation leading either to isolated cardiac conduction defect or Brugada syndrome in a large French family. *Circulation* 2001;**104**:3081–6.
27 Coronel R, Casini S, Koopmann TT, *et al.* Right ventricular fibrosis and conduction delay in a patient with clinical signs of Brugada syndrome: a combined electrophysiological, genetic, histopathologic, and computational study. *Circulation* 2005;**112**:2769–77.
28 Frustaci A, Priori S, Pieroni M, *et al.* Cardiac histological substrate in patients with clinical phenotype of Brugada syndrome. *Circulation* 2005;**112**:3680–7.
29 Postema PG, van Dessel PF, de Bakker JM, *et al.* Slow and discontinuous conduction conspire in Brugada syndrome: a right ventricular mapping and stimulation study. *Circ Arrhythm Electrophysiol* 2008;**1**:379–86.
30 Hoogendijk MG, Potse M, Vinet A, de Bakker JM, Coronel R. ST segment elevation by current-to-load mismatch: an experimental and computational study. *Heart Rhythm* 2011;**8**:111–18.
31 Hoogendijk MG, Potse M, Linnenbank AC, *et al.* Mechanism of right precordial ST-segment elevation in structural heart disease: excitation failure by current-to-load mismatch. *Heart Rhythm* 2010;**7**:238–48.
32 Hoogendijk MG, Opthof T, Postema PG, Wilde AA, de Bakker JM, Coronel R. The Brugada ECG pattern: a marker of channelopathy, structural heart disease, or neither? Toward a unifying mechanism of the Brugada syndrome. *Circ Arrhythm Electrophysiol* 2010;**3**:283–90.
33 Nademanee K, Raju H, de Noronha SV, *et al.* Fibrosis, Connexin-43, and conduction abnormalities in the Brugada syndrome. *J Am Coll Cardiol* 2015;**66**:1976–86.
34 Liang S, Lin C, Li Y, Liu T, Wang Y. L-type calcium current in right ventricular outflow tract myocytes of rabbit heart. *Sci China Life Sci* 2012;**55**:41–6.
35 Xie Y, Sato D, Garfinkel A, Qu Z, Weiss JN. So little source, so much sink: requirements for afterdepolarizations to propagate in tissue. *Biophys J* 2010;**99**:1408–15.
36 Liu CF, Cheung JW, Thomas G, Ip JE, Markowitz SM, Lerman BB. Ubiquitous myocardial extensions into the pulmonary artery demonstrated by integrated intracardiac echocardiography and electroanatomic mapping: changing the paradigm of idiopathic right ventricular outflow tract arrhythmias. *Circ Arrhythm Electrophysiol* 2014;**7**:691–700.
37 Timmermans C, Rodriguez LM, Crijns HJ, Moorman AF, Wellens HJ. Idiopathic left bundle-branch block-shaped ventricular tachycardia may originate above the pulmonary valve. *Circulation* 2003;**108**:1960–7.
38 Basso C, Ho SY, Rizzo S, Thiene G. Anatomic and histopathologic characteristics of the conductive tissues of the heart. In: Gussak I, Antzelevitch C (eds), *Electrical Diseases of the Heart.* London: Springer Verlag, 2013: pp. 47–71.
39 Basso C, Thiene G. Adipositas cordis, fatty infiltration of the right ventricle, and arrhythmogenic right ventricular cardiomyopathy. Just a matter of fat? *Cardiovasc Pathol* 2005;**14**:37–41.
40 Thiene G, Nava A, Corrado D, Rossi L, Pennelli N. Right ventricular cardiomyopathy and sudden death in young people. *N Engl J Med* 1988;**318**:129–33.
41 Basso C, Thiene G, Corrado D, Angelini A, Nava A, Valente M. Arrhythmogenic right ventricular cardiomyopathy. Dysplasia, dystrophy, or myocarditis? *Circulation* 1996;**94**:983–91.
42 Basso C, Bauce B, Corrado D, Thiene G. Pathophysiology of arrhythmogenic cardiomyopathy. *Nat Rev Cardiol* 2011;**9**:223–33.
43 Pilichou K, Thiene G, Bauce B, *et al.* Arrhythmogenic cardiomyopathy. *Orphanet J Rare Dis* 2016;**11**:33.
44 McKenna WJ, Maron B, Thiene G. Classification, epidemiology, and global burden of cardiomyopathies. *Circ Res* 2017;**121**:722–30.
45 Marra MP, Leoni L, Bauce B, *et al.* Imaging study of ventricular scar in arrhythmogenic right ventricular cardiomyopathy: comparison of 3D standard

electroanatomical voltage mapping and contrast-enhanced cardiac magnetic resonance. *Circ Arrhythm Electrophysiol* 2012;**5**:91–100.

46 Migliore F, Zorzi A, Silvano M, *et al.* Prognostic value of endocardial voltage mapping in patients with arrhythmogenic right ventricular cardiomyopathy/dysplasia. *Circ Arrhythm Electrophysiol* 2013;**6**:167–76.

47 Basso C, Ronco F, Marcus F, *et al.* Quantitative assessment of endomyocardial biopsy in arrhythmogenic right ventricular cardiomyopathy/dysplasia: an in vitro validation of diagnostic criteria. *Eur Heart J* 2008;**29**:2760–71.

48 Marcus FI, McKenna WJ, Sherrill D, *et al.* Diagnosis of arrhythmogenic right ventricular cardiomyopathy/dysplasia: proposed modification of the Task Force Criteria. *Eur Heart J* 2010;**31**:806–14.

49 Asimaki A, Tandri H, Huang H, *et al.* A new diagnostic test for arrhythmogenic right ventricular cardiomyopathy. *N Engl J Med* 2009;**360**:1075–84.

50 Basso C, Calabrese F, Angelini A, Carturan E, Thiene G. Classification and histological, immunohistochemical, and molecular diagnosis of inflammatory myocardial disease. *Heart Fail Rev* 2013;**18**:673–81.

51 Corrado D, Basso C, Leoni L, *et al.* Three-dimensional electroanatomic voltage mapping increases accuracy of diagnosing arrhythmogenic right ventricular cardiomyopathy/dysplasia. *Circulation* 2005;**111**:3042–50.

52 Corrado D, Basso C, Leoni L, *et al.* Three-dimensional electroanatomical voltage mapping and histologic evaluation of myocardial substrate in right ventricular outflow tract tachycardia. *J Am Coll Cardiol* 2008;**51**:731–9.

53 Birnie DH, Kandolin R, Nery PB, Kupari M. Cardiac manifestations of sarcoidosis diagnosis and management. *Eur Heart J* 2017;**38**:2663–70.

54 Vasaiwala SC, Finn C, Delpriore J, *et al.* Prospective study of cardiac sarcoid mimicking arrhythmogenic right ventricular dysplasia. *J Cardiovasc Electrophysiol* 2009;**20**:473–6.

55 Ladyjanskaia GA, Basso C, Hobbelink MG, *et al.* Sarcoid myocarditis with ventricular tachycardia mimicking ARVD/C. *J Cardiovasc Electrophysiol* 2010;**21**:94–8.

56 Vaseghi M, Lai C, Huang A, Fishbein MC, Shivkumar K. The relationship of the ventricular septum and right ventricular outflow tract to the right and non-coronary sinuses: implications for ablation of ventricular tachycardias. *Circulation* 2007;**116**:II–366.

57 Lerman BB. Mechanism, diagnosis, and treatment of outflow tract tachycardia. *Nat Rev Cardiol* 2015;**12**:597–608.

58 Yan GX, Antzelevitch C. Cellular basis for the Brugada syndrome and other mechanisms of arrhythmogenesis associated with ST-segment elevation. *Circulation* 1999;**100**:1660–6.

59 Catalano O, Antonaci S, Moro G, *et al.* Magnetic resonance investigations in Brugada syndrome reveal unexpectedly high rate of structural abnormalities. *Eur Heart J* 2009;**30**:2241–8.

60 Letsas KP, Efremidis M, Vlachos K, *et al.* Right ventricular outflow tract high-density endocardial unipolar voltage mapping in patients with Brugada syndrome: evidence for electroanatomical abnormalities. *Europace* 2018;**20**(FI1):f57–f63.

61 Morita H, Zipes DP, Morita ST, *et al.* Epicardial ablation eliminates ventricular arrhythmias in an experimental model of Brugada syndrome. *Heart Rhythm* 2009;**6**:665–71.

62 Brugada J, Pappone C, Berruezo A, *et al.* Brugada syndrome phenotype elimination by epicardial substrate ablation. *Circ Arrhythm Electrophysiol* 2015;**8**:1373–81.

63 Szél T, Antzelevitch C. Abnormal repolarization as the basis for late potentials and fractionated electrograms recorded from epicardium in experimental models of Brugada syndrome. *J Am Coll Cardiol* 2014;**63**:2037–45.

64 Schott JJ, Alshinawi C, Kyndt F, *et al.* Cardiac conduction defects associate with mutations in SCN5A. *Nat Genet* 1999;**23**:20–1.

65 Corrado D, Nava A, Buja G, *et al.* Familial cardiomyopathy underlies syndrome of right bundle branch block, ST segment elevation and sudden death. *J Am Coll Cardiol* 1996;**27**:443–8.

66 Migliore F, Testolina M, Zorzi A, et al. First-degree atrioventricular block on basal electrocardiogram predicts future arrhythmic events in patients with Brugada syndrome: a long-term follow-up study from the Veneto region of Northeastern Italy. *Europace* 2018 Jul **6** [Epub ahead of print]